

### 3D Simulation on turbulent flow and heat transfer behaviors in a five-start corrugated tube: Effect of depth ratio and tube modification

Narin Siriwan<sup>1)</sup>, Bopit Bubphachot<sup>1)</sup>, Smith Eiamsa-ard<sup>2)</sup>, Khwanchit Wongcharee<sup>2)</sup>, Teerapat Chompookham<sup>1)</sup> and Pitak Promthaisong<sup>\*1)</sup>

<sup>1)</sup>Heat Pipe and Thermal Tool Design Research Unit (HTDR), Faculty of Engineering, Mahasarakham University, Maha Sarakham 44150, Thailand

<sup>2)</sup>Faculty of Engineering, Mahanakorn University of Technology, Bangkok, Thailand

Received 17 March 2021

Revised 12 April 2021

Accepted 13 May 2021

#### Abstract

This paper presents a 3D simulation of turbulent flow and heat transfer behaviors in a five-start corrugated tube having depth ratios, DR = 0.02-0.16 and constant pitch ratio, PR = 1.0 and the Reynold number ranging from 5000 to 20,000. The effects of modified tubes: five-start vortex-flow corrugated tube and five-start cross corrugated tubes with different PR = 1.0-2.5 and constant DR = 0.06, were investigated. The results show that swirl flows were generated by the five-start corrugated tube with spiral wall while the five-start vortex-flow corrugated tube and five-start cross corrugated tube created a pair of vortex and multiple vortices flows, respectively. The modified tubes provided a heat transfer rates (range 26.8-172.1%) and thermal enhancement factor (range 12.6-90.8%) higher than the five-start corrugated tube. The five-start vortex-flow corrugated tube provided the highest thermal enhancement factor at 2.07 at DR=0.06, PR=1.5 and Re = 5000.

**Keywords:** Heat transfer, Friction factor, Thermal enhancement factor, Swirl flow, Corrugated tube

#### 1. Introduction

Heat exchangers have been used in many engineering applications in order to produce a compact heat exchanger with, reduced size and cost. In general, promoting fluid mixing in the tube heat exchanger by using vortex/swirl turbulators [1-5] (baffle, winglet and twisted tape etc.) and roughness tube (corrugated tube) [6-20] is one of the techniques which can increase the heat transfer through a heat exchanger tube wall without outsource energy.

In common, vortex turbulator and swirl turbulator devices generated vortex flow and spiral flow along the tube length. The flows help to disrupt the thermal boundary layer near the wall and improve heat transfer as compared to that of a tube without any turbulator. However, high pressure loss was found with using the devices leading to a greater energy usage due to higher pumping power which is undesired effect. On the other hand, corrugated tubes offer heat transfer enhancement with lower pressure loss than vortex/swirl turbulators. Therefore, the optimum tradeoff between enhanced heat transfer and increased pressure loss is an important issue for selecting and designing heat transfer enhancement devices.

Various corrugated tubes geometries were extensively tested by several researchers such as; Naphon et al. [6], Akhavan-Behabadi and Esmailpour [7], Kareem et al. [8, 9], Promthaisong et al. [10, 11], Liu et al. [12], Balla [13], Jin et al. [14, 15], Sun and Zeng [16], Wang et al. [17], Xin et al. [18], Wang et al. [19], Andrade et al. [20], Yang et al. [21] and Cao et al. [22]. Naphon et al. [6] concluded that Nusselt number and friction factor increased with higher  $x/d_i$ . On the other hand, it was observed that the factors adversely related to  $p/d_i$ , for using the single start corrugated tube. Kareem et al. [8, 9] reported that the two-start corrugated tube provided low pressure drop. In addition, they found that the three-start corrugated tube provided heat transfer ranging from 2.4-3.7 times while the friction factor slightly increased around 1.7-2.4 times, compared with the smooth tube. Promthaisong et al. [10, 11] employed two-start corrugated tube with DR = 0.02-0.16 and PR = 0.10-1.00 and five-start corrugated tube with PR = 1.0-3.5 at constant DR = 0.06. They found that the swirl flow created by the corrugated tube caused increased fluid mixing and heat transfer. The maximum TEF of two-start and five-start corrugated tube were as high as 1.16. Jin et al. [14, 15] suggested that a six-start spirally corrugated tube provided better heat transfer enhancement than four-start spirally corrugated tube. Sun and Zeng [16] reported that the corrugated tubes increased heat transfer by around 50% as compared to that of the smooth tube. A two-start spirally corrugated tube with helium (He) as the working fluid was presented by Xin et al. [18]. Wang et al. [19] used a transverse corrugated tube with different pitch to investigate the heat transfer enhancement. Yang et al. [21] investigated the heat transfer mechanism of the hybrid smooth and spirally corrugated tube. Cao et al. [22] used the corrugated tube to study the thermal characteristics with two phase flow.

In addition, many researchers attempted to improve the heat transfer rate in the corrugated tube by applying compound techniques such as; using nano-fluids as the working fluids [23-25] and using together with twisted tapes [26, 27]. In general, compound techniques can improve heat transfer and overall thermal performance as compared to an individual technique. However, pressure loss also

\*Corresponding author. Tel.: +668 6777 2646

Email address: pitak.p@msu.ac.th

doi: 10.14456/easr.2021.70

increased, especially when twisted tapes were applied. Promthaisong et al. [26, 27] reported that the use of a twisted tape in a corrugated tube resulted in a large pressure loss and thus low TEF.

The literature review suggests that tube geometry has an important role on flow mechanisms and heat transfer characteristic. From the previous works [11, 27], only few parameters of the five-start corrugated tubes were determined. An important geometric parameter including depth ratio has not reported, so far. In addition, the studies on heat transfer and flow behaviors were limited. In this work, flow and heat transfer characteristics in five-start corrugated tube were studied via 3D simulation. In addition, the effects of depth ratio was reported on flow and heat transfer behaviors were also reported. Moreover, the modified tubes: five-start vortex-flow corrugated tube and five-start cross corrugated tubes were also created and studied. To gain understanding, the 3D-structure of the fluid flow, the distributions of the temperature and local Nusselt number are presented.

## 2. Physical model of five-start corrugated tube

The system of interest is the five-start corrugated tube as shown in Figure 1. Air entered the testing duct at an inlet temperature,  $T_{in}$ . The parameter  $D$  is the characteristic diameter ( $D = 0.05$  m). The depth ratio,  $e/D$ ,  $DR = 0.02-0.16$  were investigated at constant pitch ratio,  $p/D$ ,  $PR = 1.0$  for Reynolds numbers varying from 5,000 to 20,000. For the modified tubes: the five-start vortex-flow corrugated tube and five-start cross corrugated tube are investigated at constant  $DR = 0.06$  and various  $PR$  ranging from 1.0 to 2.5.

Hexahedron grids were applied for all the computational domains. At the near wall zone (viscous sub-layer), the  $y^+ \approx 1$  was applied since momentum and temperature significantly changed.

## 3. Boundary condition

The periodic boundaries were applied at the inlet and outlet of the flow domain. The air entered with a constant mass-flow rate at 300 K ( $Pr = 0.707$ ). The physical properties of air were assumed to remain constant. The corrugated-tube wall was applied with no-slip condition and constant heat flux at  $600 \text{ W/m}^2$ .

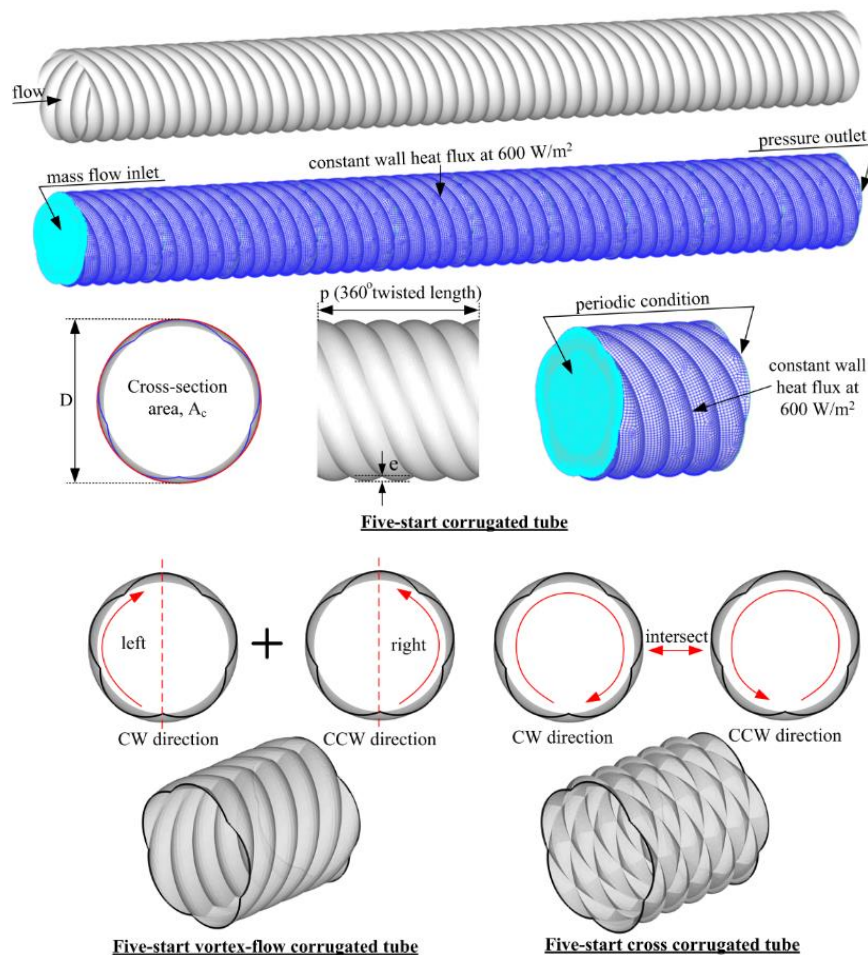


**Figure 1** Physical models of five-start corrugated tube, five-start vortex-flow corrugated tube and five-start cross corrugated tube.

## 4. Data reduction

The assumptions and phenomenon in a five-start corrugated tube for turbulent flow region and heat transfer were following: 1) incompressible flow was applied for the fluid, 2) the flow and heat transfer were steady and three-dimensional, 3) only convection heat transfer was considered in this problem (both radiation and conduction heat transfer were ignored) and 4) the body force was ignored. The governing equations under the assumptions as above, can be written as follows:

Conservation of mass equation:

$$\frac{\partial}{\partial x_i}(\rho u_i) = 0 \quad (1)$$

Conservation of momentum equation:

$$\frac{\partial}{\partial x_j}(\rho u_i u_j) = -\frac{\partial p}{\partial x_i} + \frac{\partial}{\partial x_j} \left[ \mu \left( \frac{\partial u_i}{\partial x_j} + \frac{\partial u_j}{\partial x_i} \right) - \rho \overline{u'_i u'_j} \right] \quad (2)$$

Conservation of energy equation:

$$\frac{\partial}{\partial x_j}(\rho u_i T) = \frac{\partial}{\partial x_j} \left( (\Gamma + \Gamma_t) \frac{\partial T}{\partial x_j} \right) \quad (3)$$

where  $\rho$ ,  $p$  and  $\mu$  are the density, pressure and dynamic viscosity of the fluid, respectively. The  $u_i$  is the mean component of velocity in the  $x_i$ -direction and  $u'$  is a fluctuating component of velocity. The  $\Gamma$  is a molecular thermal diffusivity and  $\Gamma_t$  is a turbulent thermal diffusivity and given by

$$\Gamma = \frac{\mu}{Pr}, \text{ and } \Gamma_t = \frac{\mu_t}{Pr_t} \quad (4)$$

The  $-\rho \overline{u'_i u'_j}$  in Eq. (2) is a Reynolds stresses and is defined in the equation below:

$$-\rho \overline{u'_i u'_j} = \mu_t \left( \frac{\partial u_i}{\partial x_j} + \frac{\partial u_j}{\partial x_i} \right) - \frac{2}{3} \left( \rho k + \mu_t \frac{\partial u_i}{\partial x_i} \right) \delta_{ij} \quad (5)$$

where the parameter,  $\delta_{ij}$ , is a Kronecker delta while the parameter,  $k$ , is the turbulent kinetic energy (TKE) and can be calculated by  $k = \frac{1}{2} \overline{u'_i u'_i}$ . For all computational domain, the Realizable  $k$ - $\epsilon$  turbulent model was used for the turbulent region. The details of the turbulent kinetic energy equation,  $k$ , and the dissipation equation,  $\epsilon$ , for the Realizable  $k$ - $\epsilon$  turbulent model were as in Ref. [10]. In this paper, the parameters are as follows:

The Reynolds number is defined as

$$Re = \frac{\rho u_0 D_h}{\mu} \quad (6)$$

The friction factor can be calculated from

$$f = \frac{(\Delta p/L) D_h}{(1/2) \rho \bar{u}^2} \quad (7)$$

The local heat transfer can be written as

$$Nu_x = \frac{h_x D_h}{k_{air}} \quad (8)$$

The area-average of the Nusselt number can be calculated from

$$Nu = \frac{1}{A} \int Nu_x \partial A \quad (9)$$

The thermal enhancement factor (TEF) is defined as

$$TEF = \frac{Nu/Nu_0}{(f/f_0)^{1/3}} \quad (10)$$

where  $Nu_0$  and  $f_0$  stand for Nusselt number and friction factor for the smooth tube, respectively.

## 5. Results and discussion

### 5.1 Validation

The computational domain was resolved by hexahedron elements. The grid independence was evaluated by determining the  $Nu$  and  $f$  values of five different grid systems: 100000, 300000, 500000, 700000 and 900000 cells. Evidently, increasing the grid number from 500000 to 700000 resulted in insignificant change of  $Nu$  and  $f$  values ( $< 0.25\%$ ). Therefore, the grid cells at about 500000 was adopted for all the computation models.

To validate the accuracy of the numerical results, the correlations [28] were used to compare with the Realizable  $k-\epsilon$  turbulent model as displayed in Figure 2. Under similar conditions, the numerical results provided mean deviations of the  $Nu$  and  $f$  of 10.1% and 6.3%, respectively. In addition, to validate the accuracy of the swirl flow using the Realizable  $k-\epsilon$  turbulent model, the smooth tube with single twisted tape inserted at  $y/w=5$  by Chokphoemphun et al. [29] was used for comparison. Under similar conditions, the results revealed that the Realizable  $k-\epsilon$  turbulent model provided good agreement with the experimental data. Both the  $Nu$  and  $f$  were less than 10% different from corresponding values in experimental data. Therefore, the Realizable  $k-\epsilon$  turbulent model was applied to the computational domain.

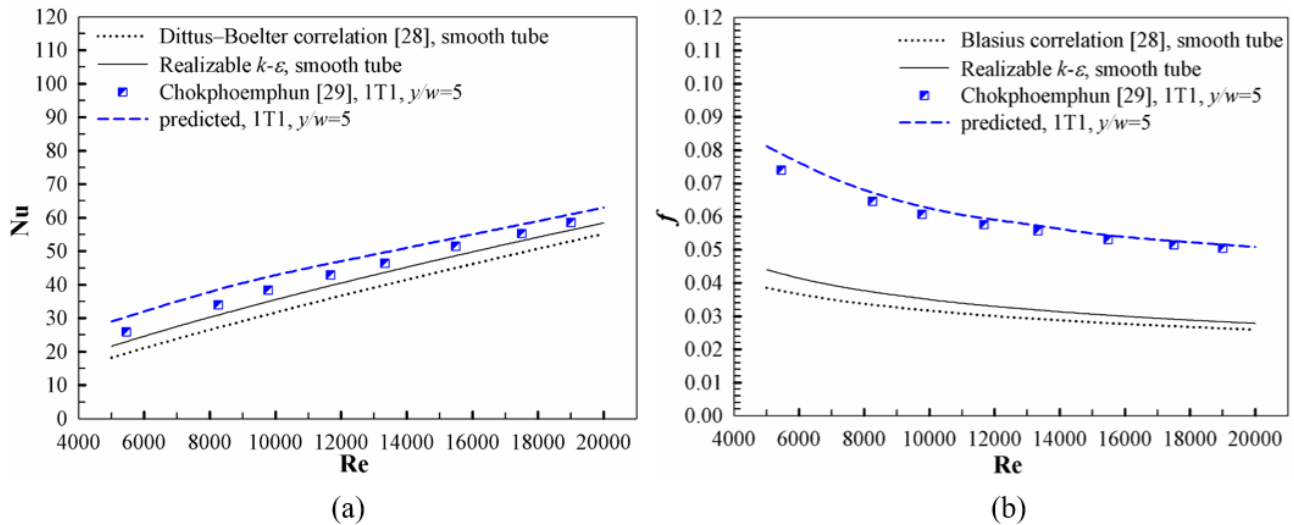


Figure 2 Verification of (a)  $Nu$  and (b)  $f$  for smooth tube and tube with swirl turbulator.

5.2 Periodic flow and heat transfer concept

Figure 3 displays the axial distribution of (a)  $u/u_0$  and (b)  $Nu/Nu_0$  at  $DR=0.06$ ,  $PR=1.0$  and  $Re=5,000$ . Evidently, two regions, a developing and a fully developed region, appeared for both the  $u/u_0$  and  $Nu/Nu_0$  profiles. For a developing region, both the  $u/u_0$  and  $Nu/Nu_0$  profiles appeared at the entry regime, and then become fully developed. The fully developed region for the  $u/u_0$  and  $Nu/Nu_0$  was found at around the 7<sup>th</sup> module ( $x/D \approx 6$ ) and 6<sup>th</sup> module ( $x/D \approx 5$ ), respectively. At fully developed periodic regime, both the flow and heat transfer appeared to have similar patterns.

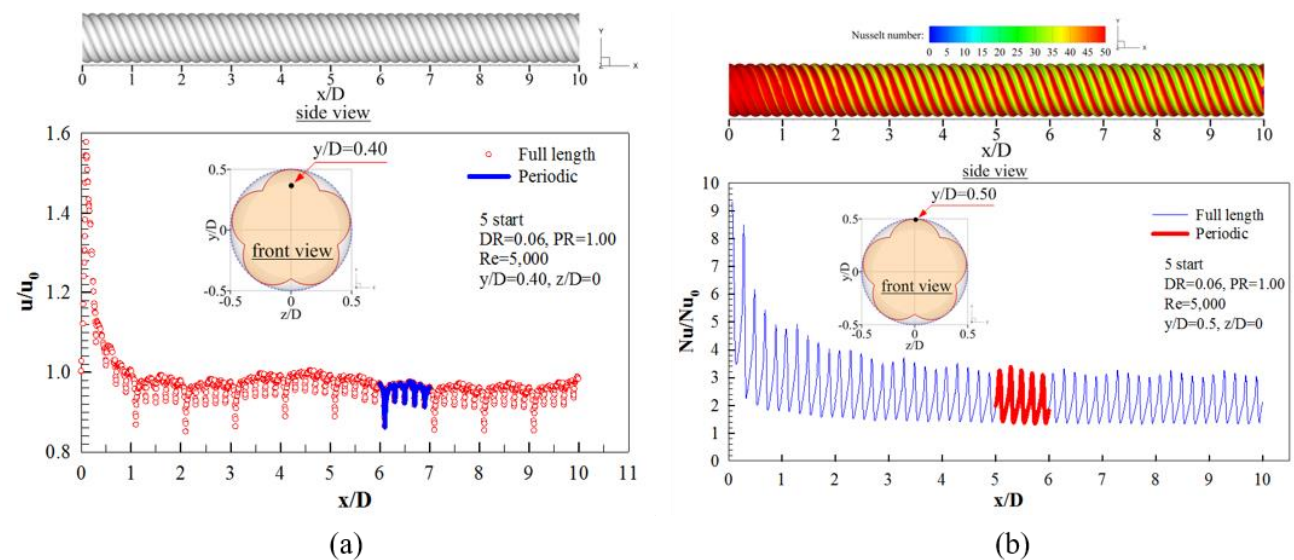


Figure 3 Axial distribution of (a)  $u/u_0$  and (b)  $Nu/Nu_0$  at  $DR=0.06$ ,  $PR=1.0$  and  $Re=5,000$ .

5.3 Flow structure

Figure 4 presents the 3D-flow structure at  $Re = 5000$ . In the figure, straight flow appeared in the smooth tube while the swirl flow was generated by the five-start corrugated tube. Secondary swirl flow appeared around the tube wall while the main swirl flow appeared at the core. However, a smaller  $DR$  value cannot create the secondary swirl flow, especially at  $DR=0.02$ . On the other hand, a higher  $DR$  value caused the secondary swirl flow to move over the groove wall, especially, at  $DR=0.16$ . For the test tube at  $PR=1.0$ , the  $DR=0.08$  can induce secondary swirl flow movement around the groove wall better than the other  $DR$  values. The swirl flow behaviors

led to accelerated flow around the tube wall which helped to disrupt the thermal boundary layer, increase fluid mixing and enhanced heat transfer to higher levels than in the smooth tube.

A comparison of the five-start corrugated tube, five-start vortex-flow corrugated tube and five-start cross corrugated tube at  $DR=0.06$ ,  $PR=1.0$  and  $Re=5000$  on 3D-flow structure were presented as iso-surfaces as displayed in Figure 5. The results indicated that different tube geometry directly affected on flow structure. The iso-surfaces flow indicated that the swirl flow around the tube wall that separated from the main swirl flow at the core was caused by the five-start corrugated tube while the five-start vortex-flow corrugated tube induced the fluid to the lower wall. Subsequently, it separated to the left and right wall around the corrugation wall. The boundary layer was drastically disrupted at the impingement zone (lower wall) due to strong vortex strength. For the five-start cross corrugated tube, multiple vortices was separated from the main flow at the core and appeared around the wall. The disruption of the boundary layer near the tube wall appeared over a larger area than that with the five-start corrugated tube. These behaviors increased the efficiency of the heat transfer enhancement.

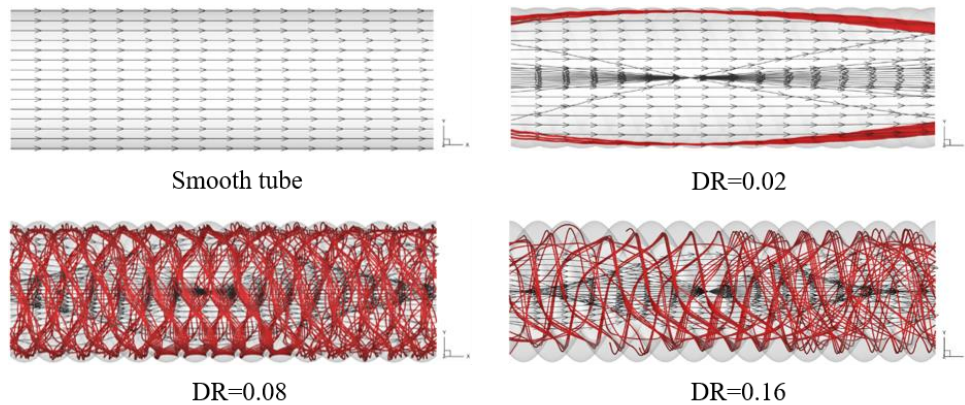


**Figure 4** 3D-Flow structure at  $PR=1.0$  and  $Re=5000$ .

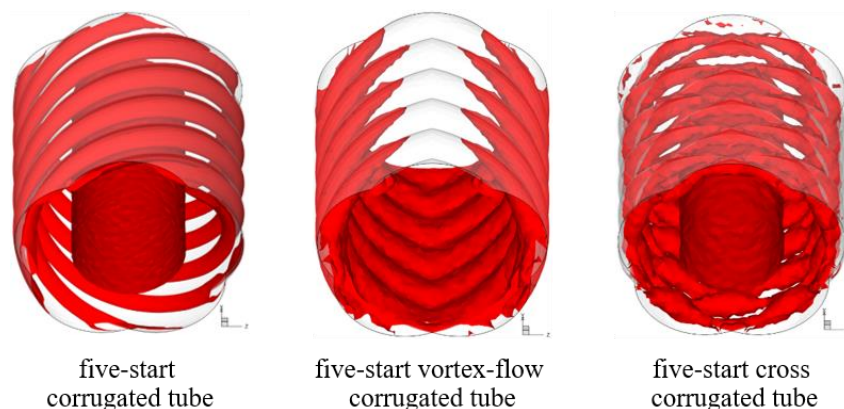


**Figure 5** Comparison of the 3D-flow structure at  $DR=0.06$ ,  $PR=1.0$  and  $Re=5000$ .

#### 5.4 Heat transfer

To understand heat transfer behaviour, the distribution of fluid temperature in the tube under test, the fluid temperature distribution in the same transverse planes and local wall Nusselt number were determined, as shown in Figures 6-9. Generally, a layer of high temperature fluid appeared near the tube wall for both the smooth tube and five-start corrugated tube at smaller  $DR$  value ( $DR=0.02$ ) while low temperature fluid was at the core as displayed in Figure 6. The layer of high temperature fluid blocked the heat transfer between the heated wall and the cold fluid, the heat transfer on the tube wall was low as shown in Figure 8. In the figure, swirl flow appears on the transverse planes. The optimum between  $DR$  and  $PR$  values with using the test tube results in reduced layer thickness of high fluid temperature regions near the tube wall better than in the other cases, especially, at  $DR=0.08$  (due to the secondary swirl flow moves around the groove wall being better than the other  $DR$  values) and gave the maximum heat transfer on the tube wall. However, higher  $DR$  values led to an increased layer of high temperature fluid due to the secondary swirl flow moving over the groove wall, resulting in the heat transfer on the tube wall being reduced, especially, at the  $DR=0.16$ .

The heat transfer behaviour of the five-start corrugated tube, five-start vortex-flow corrugated tube and five-start cross corrugated tube is presented in Figures 7 and 9. It is clearly seen that the five-start vortex-flow corrugated tube and five-start cross corrugated tube increased the levels of heat transfer over those in the five-start corrugated tube. In the figure, a pair of vortex flow was created by the five-start vortex-flow corrugated tube while multiple vortices flow appeared around the tube wall of the five-start cross corrugated tube as displayed in Figure 7. This indicated that the layer thickness of high fluid temperature regions near the tube wall was considerably reduced when compared with the five-start corrugated tube, especially the five-start vortex-flow corrugated tube. The heat transfer at the impingement zone (lower wall) was greatly increased as showed in Figure 9. In the same way, the heat transfer on the five-start cross corrugated tube wall increased caused by the multiple vortices flow around the tube wall.

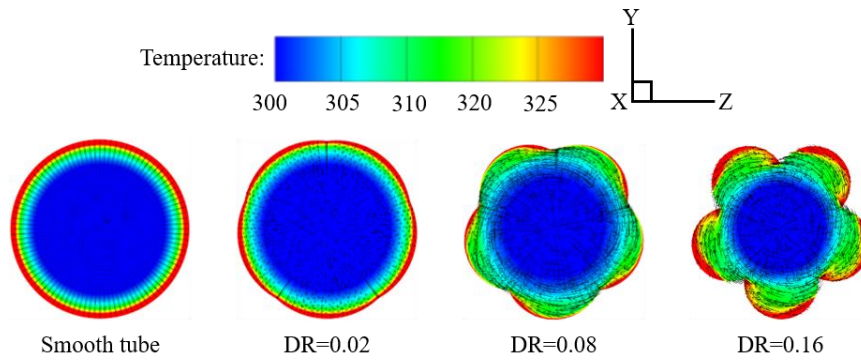


**Figure 6** Flow vector and temperature distribution in the transverse plane at PR=1.0 and Re = 5000.

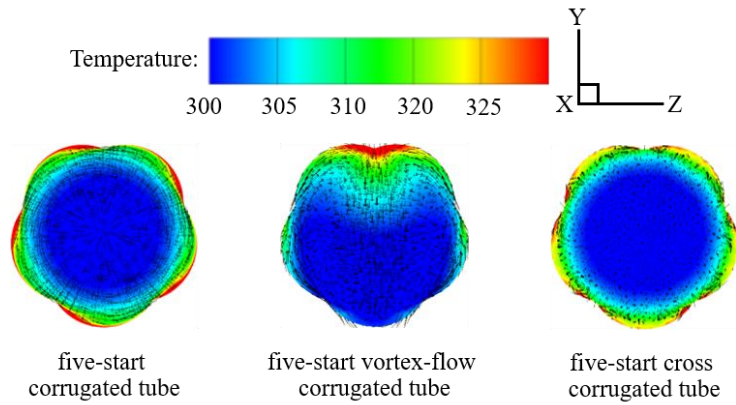


**Figure 7** Comparison of the flow vector and temperature distribution in the transverse plane at DR=0.06, PR=1.0 and Re = 5000.

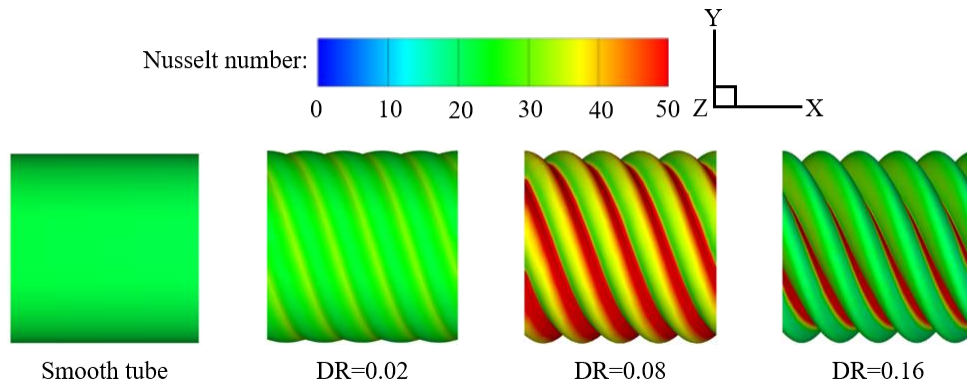


**Figure 8** Local wall Nusselt number distribution at PR=1.0 and Re = 5000.

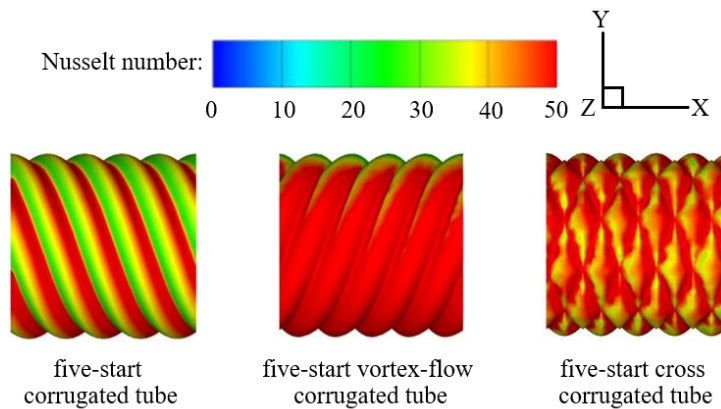


**Figure 9** Comparison of the local wall Nusselt number distribution at DR=0.06, PR=1.0 and Re = 5000.

Figure 10 (a) displays the variation of  $Nu/Nu_0$  with  $Re$  for using the five-start corrugated tube. For all cases,  $Nu/Nu_0$  are beyond unity ( $Nu/Nu_0 > 1.0$ ), except the  $DR=0.02$  and  $Re > 12,000$ . That means the five-start corrugated tube was capable of enhancing heat transfer. The  $Nu/Nu_0$  increases with increasing  $DR$  from 0.02 to 0.08 and then decreases when the  $DR > 0.08$ . The trend of the  $Nu/Nu_0$  with  $DR$  can clearly be seen in Figure 10 (d). This is because with the smaller  $DR$ , the secondary flow did not appear while at the highest  $DR$ , the fluid cannot be induced to the grooved wall. The best  $DR$  value for heat transfer enhancement using the test tube at  $PR=1.0$  was the  $DR=0.08$ . In the range investigated, the  $Nu/Nu_0$  was found in the range 0.92-2.04. The  $DR=0.08$  provided the highest  $Nu/Nu_0$  at 2.04 at the lowest  $Re$ .

The variation of  $f/f_0$  with  $Re$  is presented in Figure 10 (b). For all cases,  $f/f_0$  was above unity ( $f/f_0 > 1.0$ ). That means the five-start corrugated tube caused extra friction losses compared with the smooth tube. The increase of  $DR$  led to an increase in the  $f/f_0$  due to the flow blockage increasing. In the range investigated, the five-start corrugated tube gave  $f/f_0$  in the range 1.45-11.33. The  $DR=0.16$  gave the highest  $f/f_0$  at 11.33 at the lowest  $Re$ .

Figure 10 (c) presents the relationship between the TEF and  $Re$ . In the figure, increasing  $Re$  led to decreasing TEF for all cases. In the range studied, the  $DR=0.06$  yields the highest TEF of 1.10 at  $Re = 5000$ .

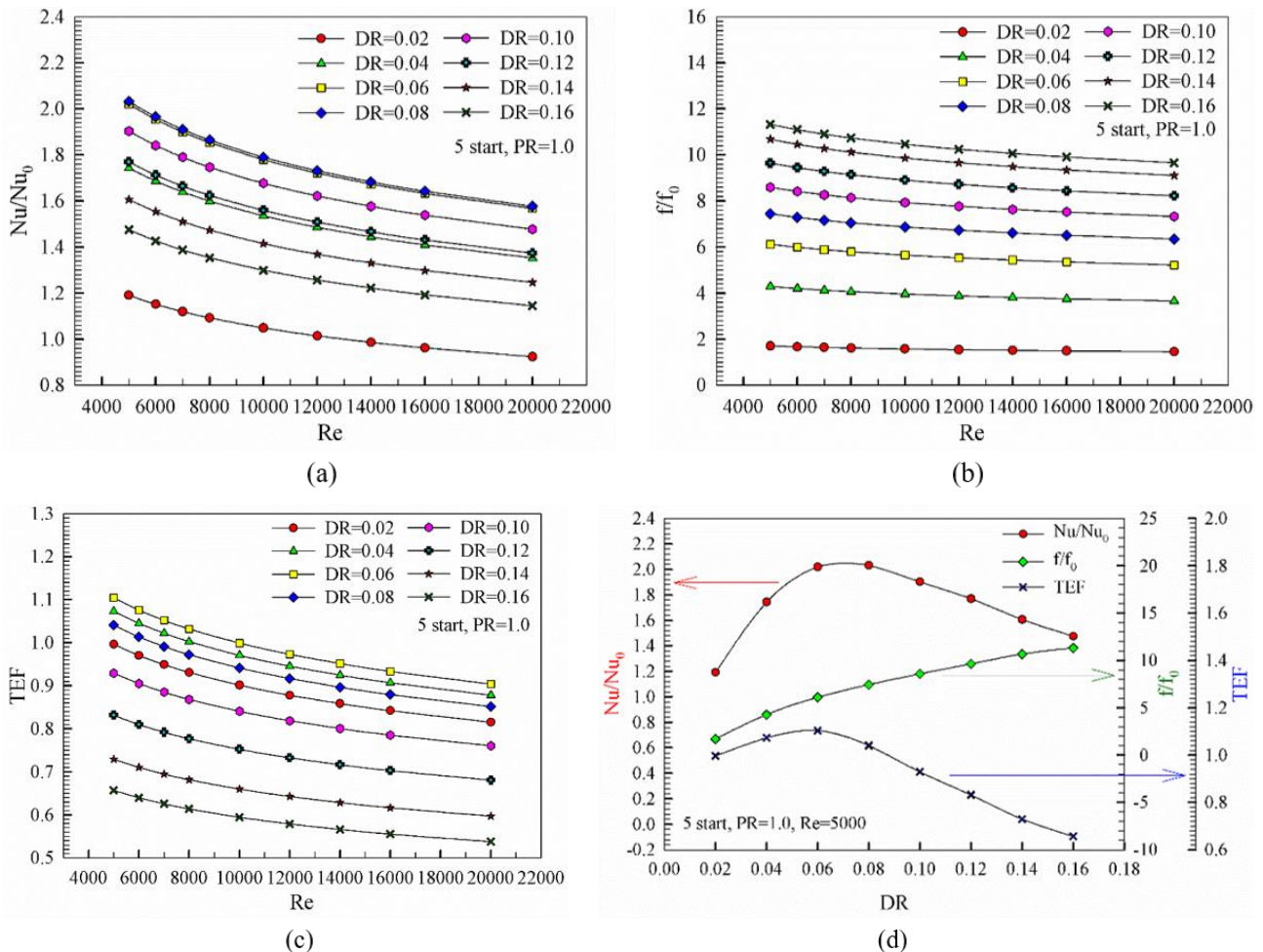


**Figure 10** Variation of (a)  $Nu/Nu_0$ , (b)  $f/f_0$ , (c) TEF with  $Re$  and (d)  $Nu/Nu_0$ ,  $f/f_0$ , TEF with  $DR$  for the five-start corrugated tube.

Figure 11 displays the variation of  $Nu/Nu_0$ ,  $f/f_0$  and TEF with  $PR$  at various  $Re$  for the five-start corrugated tube, five-start vortex-flow corrugated tube and five-start cross corrugated tube at only  $DR=0.06$  (due to give the highest TEF for the five-start corrugated tube). The  $PR=1.0-2.5$  were investigated for the modified tube. In the figure, both the five-start vortex-flow corrugated tube and five-start cross corrugated tube resulted in the  $Nu/Nu_0$  being higher than in the five-start corrugated tube for all  $PR$ , and the five-start vortex-flow corrugated tube gave the  $Nu/Nu_0$  higher than the five-start cross corrugated tube for all  $PR$ . Increasing  $PR$  results in a decrease in the  $Nu/Nu_0$  because of the vortex strength decay. In the range investigated, the five-start vortex-flow corrugated tube and five-start cross corrugated tube provided the  $Nu/Nu_0$  range of 2.49-4.2 and 1.9-3.57, which were higher than that of the five-start corrugated tube at around 51.5-118.6% and 15.6-86.1%, respectively.

When considering the  $f/f_0$ , at the same  $PR$  ( $PR=1.0$ ), both the five-start vortex-flow corrugated tube and five-start cross corrugated tube provided the  $f/f_0$  higher than the five-start corrugated tube around 36.3-172.1% and 26.8-153.1%, respectively, due to higher flow blockage. Increasing  $PR$  led to decrease  $f/f_0$ . In the range investigated, the five-start vortex-flow corrugated tube and five-start cross corrugated tube provided the  $f/f_0$  range of 4.72-14.2 and 3.85-13.2, respectively. The maximum  $f/f_0$  was found at 14.2 for the five-start vortex-flow corrugated tube at  $DR=0.06$ ,  $PR=1.0$  and  $Re=20,000$ .

When considering the TEF, it clearly seen that both the five-start vortex-flow corrugated tube and five-start cross corrugated tube increased the TEF higher than that of the five-start corrugated tube for all PR. The TEF for the five-start vortex-flow corrugated tube and five-start cross corrugated tube was found around 1.24-2.07 and 1.05-1.8, respectively, and was higher than the five-start corrugated tube at around 37.8-90.8% and 12.6-66.9%, respectively. For all PR, the five-start vortex-flow corrugated tube provided the TEF higher than the five-start cross corrugated tube due to more efficient heat transfer enhancement. The maximum TEF was found at PR=1.5 for the modified tube. The suggest case was the five-start vortex-flow corrugated tube at DR=0.06 and PR=1.5 due to provide the highest TEF around 2.07 at the lowest Re.

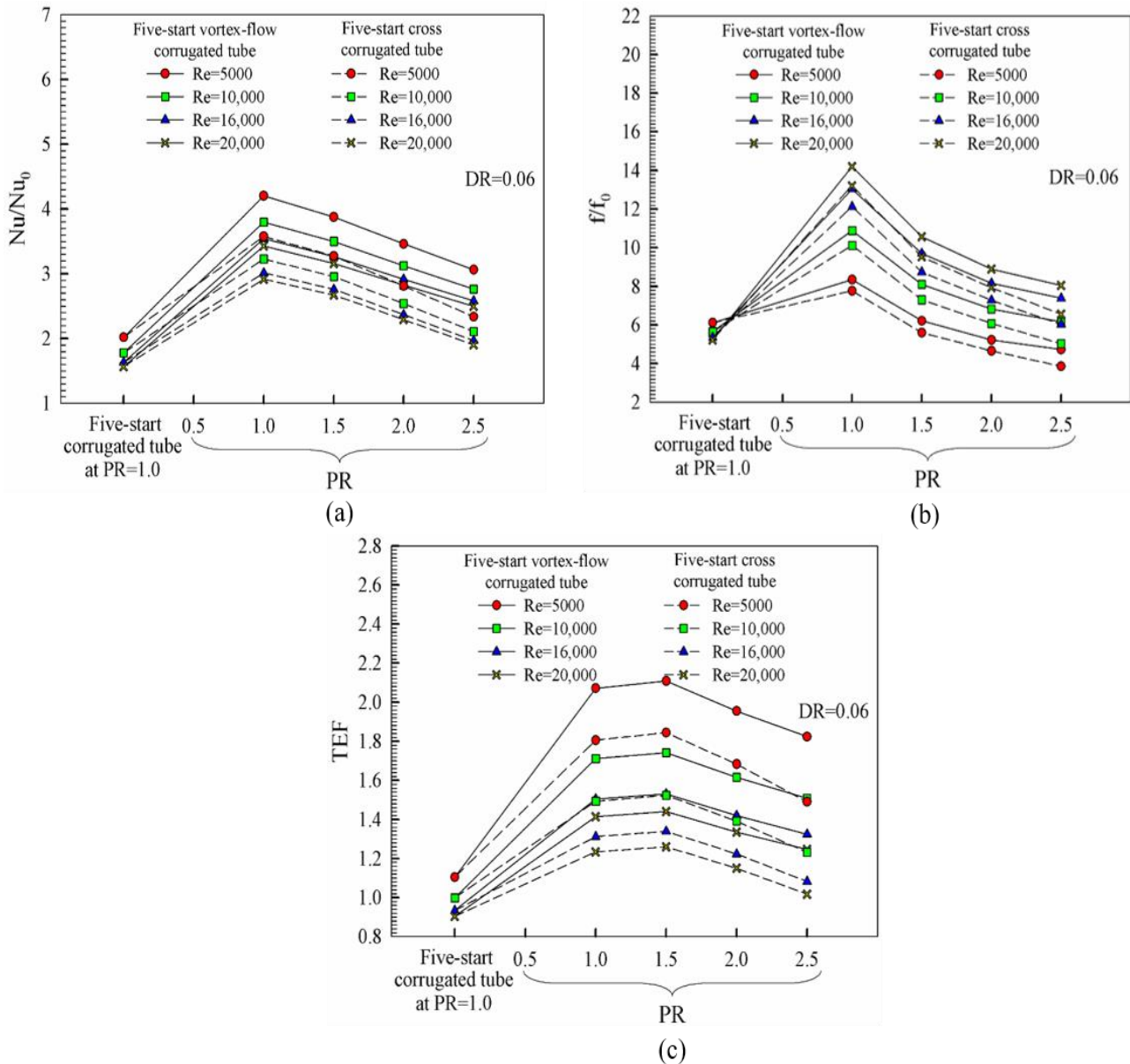


**Figure 11** Variation of (a)  $Nu/Nu_0$ , (b)  $f/f_0$  and (c) TEF with PR at various Re for the five-start corrugated tube, five-start vortex-flow corrugated tube and five-start cross corrugated tube at DR=0.06.

**6. Comparison with previous work**

Figure 12 present a comparison of TEF values from previously published investigations. The maximum TEF is reported from the current work and previous work such as; inclined vortex rings [1], staggered-winglet perforated-tapes [2], V-shaped baffles [5], three-start spirally twisted tube combined with triple-channel twisted tape in belly-to-neck arrangement [26] and five-start spiral corrugated tube combined with five-channel twisted taped [27]. In the figure, the five-start vortex-flow corrugated tube give a much higher TEF than both the vortex turbulator and the corrugated tube combined with the twisted tape due to lower friction loss, except; the V-shaped baffles. Thus, from the viewpoint of energy savings, high thermal enhancement factors given by five-start vortex-flow corrugated tube are the result of low friction factors.

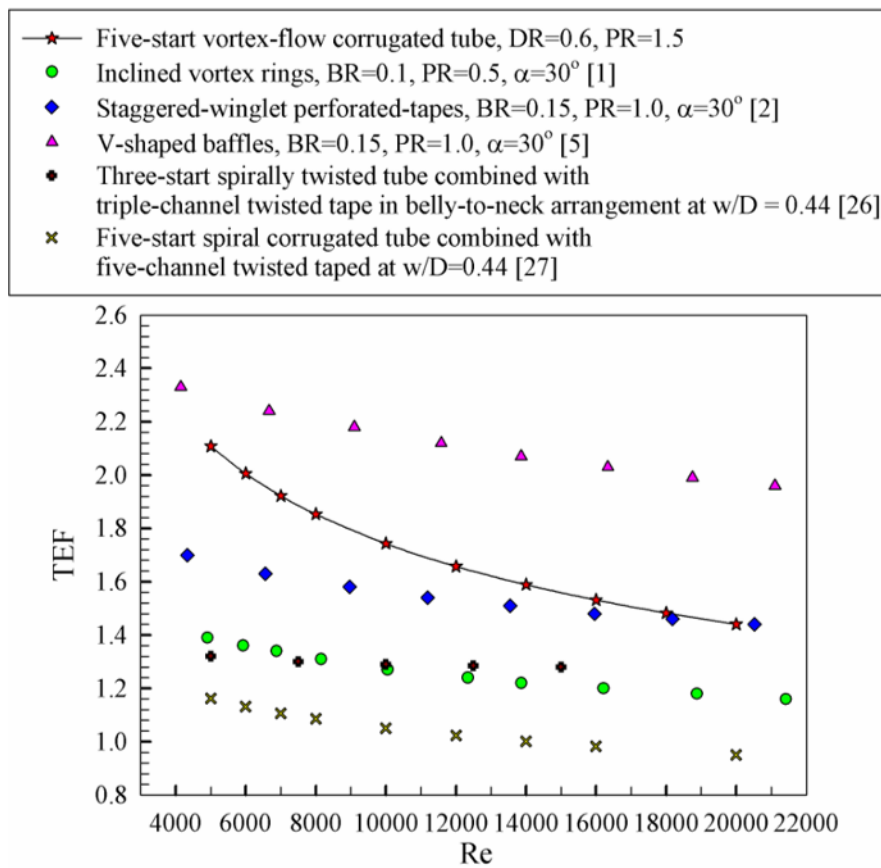


**Figure 12** Comparison of the TEF with the previous work.

## 7. Conclusions

The effects of a five-start corrugated tube on heat transfer enhancement, pressure drop and thermal enhancement factor with different depth ratios,  $DR = 0.02-0.16$  at constant pitch ratios,  $PR = 1.0$  were investigated in turbulent flow,  $Re=5000-20,000$ . Two type of five-start corrugated tube modification; five-start vortex-flow corrugated tube and five-start cross corrugated tube were studied on flow and heat transfer behaviors at constant  $DR=0.06$  and various  $PR=1.0-2.5$ . The main findings can be concluded as follows:

1. The fully developed regions for the  $u/u_0$  and  $Nu/Nu_0$  were found at around the 7<sup>th</sup> module ( $x/D \approx 6$ ) and 6<sup>th</sup> module ( $x/D \approx 5$ ), respectively.

2. The five-start corrugated tube creates swirl flows while the five-start vortex-flow corrugated tube and five-start cross corrugated tube generated a pair vortex flow and multiple vortices flow, respectively, which help to promote the mixing of the fluid in the tube and thus enhancing heat transfer between the fluid and the tube wall.

3. The  $DR=0.06$  was the optimum point for the five-start corrugated tube at  $PR=1.0$  due to it providing the maximum TEF when compared with other  $DR$ .

4. The five-start vortex-flow corrugated tube and five-start cross corrugated tube provided the  $Nu/Nu_0$  higher than the five-start corrugated tube around 51.5-118.6% and 15.6-86.1%, respectively, and 37.8-90.8% and 12.6-66.9%, respectively, for the TEF.

5. In the rang studied, the suggested case was the five-start vortex-flow corrugated tube due to provide the highest TEF at about 2.07 at  $DR=0.06$ ,  $PR=1.5$  and  $Re=5000$ .

## 8. Acknowledgements

This research was financially supported by Faculty of Engineering Maharakham University (Grant year 2021).

## 9. References

- [1] Promvong P, Koolnapadol N, Pimsarn M, Thianpong C. Thermal performance enhancement in a heat exchanger tube fitted with inclined vortex rings. *Appl Therm Eng.* 2014;62(1):285-92.
- [2] Skullong S, Promvong P, Thianpong C, Pimsarn M. Heat transfer and turbulent flow friction in a round tube with staggered-winglet perforated-tapes. *Int J Heat Mass Tran.* 2016;95:230-42.
- [3] Nanan K, Thianpong C, Pimsarn M, Chuwattanakul V, Eiamsa-ard S. Flow and thermal mechanisms in a heat exchanger tube inserted with twisted cross-baffle turbulators. *Appl Therm Eng.* 2017;114:130-47.
- [4] Promvong P, Skullong S. Thermo-hydraulic performance in heat exchanger tube with v-shaped winglet vortex generator. *Appl Therm Eng.* 2020;164:114424.
- [5] Promvong P, Skullong S. Enhanced thermal performance in tubular heat exchanger contained with v-shaped baffles. *Appl Therm Eng.* 2021;185:116307.

- [6] Naphon P, Nuchjapo M, Kurujareon J. Tube side heat transfer coefficient and friction factor characteristics of horizontal tube with helical rib. *Energy Convers Manag.* 2006;47:3031-44.
- [7] Akhavan-Behabadi MA, Esmailpour M. Experimental study of evaporation heat transfer of R-134a inside a corrugated tube with different tube inclinations. *Int Comm Heat Mass Tran.* 2014;55:8-14.
- [8] Kareem ZS, Mohd Jaafar MN, Lazim TM, Abdullah S, AbdulWahid AF. Heat transfer enhancement in two-start spirally corrugated tube. *Alexandria Eng J.* 2015;54(3):415-22.
- [9] Kareem ZS, Abdullah S, Lazim TM, Mohd Jaafar MN, AbdulWahid AF. Heat transfer enhancement in three start spirally corrugated tube: experimental and numerical study. *Chem Eng Sci.* 2015;134:746-57.
- [10] Promthaisong P, Jedsadaratanachai W, Eiamsa-ard S. 3D Numerical study on the flow topology and heat transfer characteristics of turbulent forced convection in spirally corrugated tube. *Numer Heat Tran Appl.* 2016;69:607-29.
- [11] Promthaisong P, Jedsadaratanachai W, Chuwattanakul V, Eiamsa-ard S. Heat transfer and fluid flow behaviors in a five-start spiral corrugated tube. *AIP Conf Proc.* 2017;1879(1):020005.
- [12] Liu JJ, Liu ZC, Liu W. 3D numerical study on shell side heat transfer and flow characteristics of rod-baffle heat exchangers with spirally corrugated tubes. *Int J Therm Sci.* 2015;89:34-42.
- [13] Balla HH. Enhancement of heat transfer in six-start spirally corrugated tubes. *Case Stud Therm Eng.* 2017;9:79-89.
- [14] Jin ZJ, Liu BZ, Chen F Q, Gao ZX, Gao XF, Qian JY. CFD analysis on flow resistance characteristics of six-start spirally corrugated tube. *Int J Heat Mass Tran.* 2016;103:1198-20.
- [15] Jin ZJ, Chen FQ, Gao ZX, Gao XF, Qian JY. Effects of pitch and corrugation depth on heat transfer characteristics in six-start spirally corrugated tube. *Int J Heat Mass Tran.* 2017;108:1011-25.
- [16] Sun M, Zeng M. Investigation on turbulent flow and heat transfer characteristics and technical economy of corrugated tube. *Appl Therm Eng.* 2018;129:1-11.
- [17] Wang W, Zhang Y, Liu J, Li B, Sunden B. Numerical investigation of entropy generation of turbulent flow in a novel outward corrugated tube. *Int J Heat Mass Tran.* 2018;126:836-47.
- [18] Xin F, Liu Z, Zheng N, Liu P, Liu W. Numerical study on flow characteristics and heat transfer enhancement of oscillatory flow in a spirally corrugated tube. *Int J Heat Mass Tran.* 2018;127:402-13.
- [19] Wang G, Qi C, Liu M, Li C, Yan Y, Liang L. Effect of corrugation pitch on thermo-hydraulic performance of nanofluids in corrugated tubes of heat exchanger system based on exergy efficiency. *Energy Convers Manag.* 2019;186:51-65.
- [20] Andrade A, Moita AS, Nikulin A, Moreira ALN, Santos H. Experimental investigation on heat transfer and pressure drop of internal flow in corrugated tubes. *Int J Heat Mass Tran.* 2019;140:940-55.
- [21] Yang C, Liu G, Zhang J, Qi JY. Thermohydraulic analysis of hybrid smooth and spirally corrugated tubes. *Int J Therm Sci.* 2020;158:106520.
- [22] Cao Y, Nguyen PT, Jernsittiparsert K, Belmabrouk H, Alharbi SO, khorasani MS. Thermal characteristics of air-water two-phase flow in a vertical annularly corrugated tube. *J Energy Storage.* 2020;31:101605.
- [23] Rabienataj Darzi AA, Farhadi M, Sedighi K, Shafaghat R, Zabihi K. Experimental investigation of turbulent heat transfer and flow characteristics of SiO<sub>2</sub>/water nanofluid within helically corrugated tubes. *Int J Heat Mass Tran.* 2012;39:1425-34.
- [24] Rabienataj Darzi AA, Farhadi M, Sedighi K, Aallahyari S, Delavar MA. Turbulent heat transfer of Al<sub>2</sub>O<sub>3</sub>-water nanofluid inside helically corrugated tubes: numerical study. *Int J Heat Mass Tran.* 2013;41:68-75.
- [25] Rabienataj Darzi AA, Farhadi M, Sedighi K. Experimental investigation of convective heat transfer and friction factor of Al<sub>2</sub>O<sub>3</sub>/water nanofluid in helically corrugated tube. *Exp Therm Fluid Sci.* 2014;57:188-99.
- [26] Eiamsa-ard S, Promthaisong P, Thianpong C, Pimsarn M, Chuwattanakul V. Influence of three-start spirally twisted tube combined with triple-channel twisted tape insert on heat transfer enhancement. *Chem Eng Process.* 2016;102:117-29.
- [27] Promthaisong P, Jedsadaratanachai W, Chuwattanakul V, Eiamsa-ard S. Simulation of turbulent heat transfer characteristics in a corrugated tube with five-channel twisted tape inserts. *AIP Conf Proc.* 2017;1879(1):020004.
- [28] Incropera F, Dewitt PD, Bergman TL, Lavine AS. Introduction to heat transfer. 6<sup>th</sup> ed. New Jersey: John Wiley & Sons Inc; 2006.
- [29] Chokphoemphun S, Pimsarn M, Thianpong C, Promvong P. Heat transfer augmentation in a circular tube with winglet vortex generators. *Chin J Chem Eng.* 2015;23:755-62.